Neurovascular factors in resting-state functional MRI

Thomas T. Liu[*]
Center for Functional Magnetic Resonance Imaging, University of California San Diego, 9500 Gilman Drive, MC 0677, La Jolla, CA 92093-0677, USA; Department of Radiology, University of California San Diego, 9500 Gilman Drive, MC 0677, La Jolla, CA 92093-0677, USA; Department of Bioengineering, University of California San Diego, 9500 Gilman Drive, MC 0677, La Jolla, CA 92093-0677, USA

Thomas T. Liu: ttliu@ucsd.edu

Abstract

There has been growing interest in the use of resting-state functional magnetic resonance imaging (rsfMRI) for the assessment of disease and treatment, and a number of studies have reported significant diseaserelated changes in resting-state blood oxygenation level dependent (BOLD) signal amplitude and functional connectivity. rsfMRI is particularly suitable for clinical applications because the approach does not require the patient to perform a task and scans can be obtained in a relatively short amount of time. However, the mechanisms underlying resting-state BOLD activity are not well understood and thus the interpretation of changes in resting state activity is not always straightforward. The BOLD signal represents the hemodynamic response to neural activity, and changes in resting-state activity can reflect a complex combination of neural, vascular, and metabolic factors. This paper examines the role of neurovascular factors in rsfMRI and reviews approaches for the interpretation and analysis of resting state measures in the presence of confounding factors.

Keywords

Neurovascular coupling; BOLD; fMRI; Functional connectivity

Introduction

Measures of resting-state functional connectivity based on the blood oxygenation level dependent (BOLD) signal have the potential to significantly enhance the diagnosis and treatment of disease (Fox and Raichle, 2007). Because they do not require the performance of a task, resting state BOLD measures can be more readily integrated into clinical protocols as compared to more traditional task-related BOLD measures. Indeed, a growing number of resting-state functional magnetic resonance imaging (rsfMRI) studies are demonstrating that resting-state connectivity measures may serve as a sensitive marker of disease. For example, with Alzheimer's disease, a range of studies has found reduced connectivity in various resting-state networks (Allen et al., 2007; Greicius et al., 2004; He et al., 2007; Li et al., 2002; Liu et al., 2008; Sorg et al., 2007; Wang et al., 2006, 2007). These decreases in resting-state BOLD connectivity are typically interpreted as an impairment of the neural connections between functionally related brain regions. However, it is critical to note that the interpretation of such studies is complicated by the fact that some diseases, such as

[*]UCSD Center for Functional MRI, 9500 GilmanDrive, MC0677, LaJolla, CA92093-0677, USA. Fax: +1 858 822 0605.

Alzheimer's disease, are likely to lead to changes in both neural connectivity and neurovascular coupling (Iadecola, 2004). As the BOLD signal reflects the hemodynamic response to neural activity (Buxton et al., 2004), factors that reduce the neurovascular coupling between neural fluctuations and the BOLD signal can diminish the amplitude of BOLD signal fluctuations, leading to a decrease in the correlation between resting-state BOLD fluctuations from different brain regions without a concomitant decrease in the neural connectivity. The overall situation is depicted in Fig. 1, in which the correlation r between the measured BOLD fluctuations from regions 1 and 2 depends on both the correlation ρ between neural power fluctuations in these regions and the neurovascular coupling between neural and BOLD fluctuations. There are also additional noise components that will be discussed in a later section. In addition to disease, other factors, such as drugs, anesthesia, medication, and variations in individual physiology, can cause changes in neurovascular coupling and modulate measures of resting-state connectivity (Greicius et al., 2008; Khalili-Mahani et al., 2012; Kiviniemi et al., 2005; Li et al., 2000; Peltier and Shah, 2011; Wong et al., 2012).

The goal of this paper is to provide an overview of the role of neurovascular coupling in rsfMRI studies. The paper will primarily review studies involving pharmacological factors in which the relatively well controlled modulation of the neurovascular state facilitates interpretation. After a brief review of the basic BOLD signal model and the normalization and calibration approaches that have been previously developed for task-related fMRI, I will discuss how these models and approaches can be extended to the analysis and interpretation of rsfMRI studies. I will also touch upon the controversial role of global signal regression in rsfMRI studies and discuss the use of multimodal measures for better understanding the relative contributions of neural and vascular factors to rsfMRI measures of connectivity.

Neurovascular coupling and the task-related BOLD signal

Before addressing the issues with the interpretation of rsfMRI studies, we briefly review the role of neurovascular coupling within the context of task-related fMRI, where the issue has been extensively considered by a number of investigators. The term *neurovascular coupling* is used to broadly describe the link between neural activity and the hemodynamic changes that give rise to the BOLD signal. To date, most functional magnetic resonance imaging (fMRI) studies have implicitly interpreted the blood oxygenation level dependent (BOLD) signal as a measure of neural activity. However, the BOLD signal does not directly measure neural activity, but rather reflects the complex interplay of neural, vascular, and metabolic processes (Buxton et al., 2004). Specifically, neuronal activation gives rise to changes in cerebral blood flow (CBF), the cerebral metabolic rate of oxygen ($CMRO_2$), and cerebral blood volume (CBV). These factors then modulate the deoxyhemoglobin (dHb) content of the brain microvasculature, perturbing the magnetic field within and around blood vessels and thus altering the local magnetic resonance signal.

Although the mechanisms that underlie the BOLD signal are still under investigation, most task-related fMRI studies interpret differences (e.g., between conditions, subjects, or populations) in the BOLD signal as differences in neural activity. While this interpretation is reasonable for studies of a specific brain region in healthy young subjects, the validity of the BOLD signal as a measure of neural activity is less well established when comparing the signal across brain regions, subjects, or conditions in which there may be significant variations in physiology. Indeed, there has been a growing appreciation that changes in neurovascular coupling, due to factors such as disease, age, and medication, can significantly alter the task-related BOLD response (Carusone et al., 2002; D'Esposito et al., 2003; Iannetti and Wise, 2007; Lindauer et al., 2010). For example, Cohen et al. (2002) demonstrated that changes in baseline cerebral blood flow could significantly alter both the

amplitude and shape of the BOLD response. In subsequent work Behzadi and Liu (2005) demonstrated that the observed changes in the BOLD response could be accounted for by changes in the biomechanical dynamics of the vascular system without any underlying change in neural activity.

In an effort to address variations in neurovascular coupling, two main approaches have been proposed for making the task-related BOLD signal a more accurate reflection of neural activity within the context of human fMRI studies. The first approach uses normalization to remove variability in the BOLD signal that is primarily due to differences in baseline vascular and metabolic factors. In this approach, an additional measure that is considered to be unrelated to neural activity is acquired and used to account for the variability in the BOLD signal. For example, the functional BOLD response amplitude can be normalized (typically through division) by the BOLD response to hypercapnia (Biswal et al., 2007; Cohen et al., 2004; Handwerker et al., 2007; Thomason et al., 2007) or measures of baseline CBF and venous oxygenation (Liau and Liu, 2009; Lu et al., 2010). Of particular relevance in this paper, resting-state BOLD amplitudes have also been used to normalize task-related BOLD response amplitudes (Biswal et al., 2007; Kannurpatti and Biswal, 2008).

In the second main approach, combined measures of BOLD and CBF signals are used to estimate functional changes in $CMRO_2$. In animal models, $CMRO_2$ measures have been shown to strongly reflect changes in neuronal firing rates, even in the presence of large modulations of the baseline neural and vascular states (Maandag et al., 2007; Smith et al., 2002). For human studies, a practical approach uses the BOLD signal model described by Davis et al. (1998) and based on the seminal work of Ogawa et al. (1993). As compared to a typical fMRI experiment which requires only measures of the task-related BOLD response, this approach requires the additional acquisition of the task-related CBF response (obtained using arterial spin labeling MRI) as well as measures of the BOLD and CBF responses to gas manipulations, such as hypercapnia and hyperoxia (Gauthier et al., 2012).

In the BOLD signal model, the fractional BOLD signal change (δ/S_0) is related to the underlying changes in cerebral blood flow (CBF) and the cerebral metabolic rate of oxygen ($CMRO_2$) through the following equation:

$$b = \frac{\Delta S}{S_0} = M(1 - f^{\alpha-\beta}m^{\beta}) \quad (1)$$

where $f = CBF/CBF_0$ and $m = CMRO_2/CMRO_{2,0}$ represent the physiological quantities normalized by their respective baseline values. The unitless parameter M defines the maximum possible BOLD signal change for a brain region and can be written as $M = A \cdot CBV_0 \cdot TE \cdot [dHB]_0^{\beta}$ where A is a multiplicative factor that depends on magnetic field strength, CBV_0 is the baseline blood volume, TE denotes echo time, and $[dHB]_0$ is the baseline concentration of deoxyhemoglobin (Hoge et al., 1999a). The additional parameters are determined empirically but are well approximated as $\alpha \approx 0.4$ and $\beta \approx 1.5$ (Buxton et al., 2004). To characterize how the balance of changes in CBF and $CMRO_2$ affects the BOLD signal, it is also useful to define a ratio $n = (f-1)/(m-1)$ that reflects the strength of the coupling between the CBF and $CMRO_2$ changes (Hoge et al., 1999b).

The original Davis approach uses measurements of the BOLD and CBF responses to a hypercapnic challenge (e.g., inhalation of 5% CO_2) to estimate the parameter M and then uses the functional BOLD and CBF responses to estimate the functional $CMRO_2$ response. More recent developments of the method include additional gas challenges, such as hyperoxia and simultaneous hyperoxia and hypercapnia (Chiarelli et al., 2007; Gauthier and

Hoge, 2012; Gauthier et al., 2012). These newer methods also enable the quantification of resting state $CMRO_2$ levels and the estimate of absolute changes in the functional $CMRO_2$ responses, whereas the Davis method is limited to estimates of relative $CMRO_2$ changes.

Although calibration approaches have the potential to offer a deeper interpretation of fMRI studies, their application has been somewhat limited by the added experimental and technical complexities of the method. In contrast, normalization approaches have the advantage of being easier to apply and integrate into existing studies, but offer more limited information. An extensive review of the application and limitation of normalization and calibration approaches for task-related fMRI is provided in Liu et al. (2013).

Neurovascular coupling in the resting state

Although there are limited studies on the subject, the dependence of the BOLD signal on changes in flow and metabolism in the resting state appears to be similar to the relation observed for evoked responses. Fukunaga et al. (2008) examined the ratio of the root mean square (RMS) amplitudes of BOLD and CBF fluctuations in the visual cortex and found similar values of the ratios during visual stimulus and rest, suggesting a similar metabolic component in the two states. Rack-Gomer (2011) examined the relation across subjects between BOLD and CBF RMS amplitudes during both a motor task and rest. Using the calibrated fMRI approach of Davis et al. (1998) to estimate the relative coupling ratio n between CBF and $CMRO_2$ changes (described in greater detail below), she found evidence for tighter coupling during the rest state as compared to the motor task state. The lower coupling ratio estimated for the rest state was similar to the ratios observed for cognitive paradigms and brain regions with relatively weak task-related responses, such as the memory encoding response in the medial temporal lobe (Restom et al., 2008). Wu et al. (2009) used the Davis model to estimate resting-state $CMRO_2$ time courses and demonstrated that the resulting functional connectivity maps were similar to those obtained using BOLD and CBF time courses. It should be noted that because the resting state BOLD amplitudes were much smaller than the assumed maximal BOLD response parameter M used in the model, the $CMRO_2$ estimates were dominated by the CBF responses (Restom et al., 2008), resulting in a strong spatial similarity between the $CMRO_2$ and CBF functional connectivity maps.

The prior studies suggest that the Davis model serves as a reasonable framework for understanding the effect of the neurovascular state on both task-related and resting-state BOLD signals. In the signal model of Eq. (1), the BOLD signal depends on both the baseline parameter M and the balance between functional changes in CBF and $CMRO_2$, with the BOLD signal amplitude rising with increases in CBF and decreases in $CMRO_2$. As noted above, the balance between CBF and $CMRO_2$ changes is often characterized by the CBF/$CMRO_2$ coupling ratio n. Changes in baseline blood volume or oxygenation can alter the parameter M and thereby modulate the amplitude of the BOLD response. Panel (A) of Fig. 2 shows examples of the BOLD versus CBF response amplitudes for different values of the parameter M and an assumed coupling factor of $n = 2.5$. For each curve, the BOLD response increases monotonically with the CBF response, with the parameter M acting as an overall scaling factor. Panel (B) of Fig. 2 shows the BOLD versus CBF response amplitudes for several coupling factors and an assumed scaling factor of $M = 8.0\%$. For finite and positive values of the coupling factor, decreases in the coupling factor indicate a tighter coupling between the CBF and $CMRO_2$ responses. For any given percent CBF increase, this results in a relatively greater $CMRO_2$ response and hence a smaller BOLD signal, as evidenced by the downward shift in the curves with decreasing values of n. The curve associated with $n = \infty$ reflects the response to a hypercapnic challenge, which is assumed to induce an increase in CBF without affecting $CMRO_2$.

Using the BOLD signal model to interpret changes in resting-state BOLD amplitude

As an example of how the BOLD signal model can be used to interpret rsfMRI results, we first consider the effects of caffeine, which has been shown to reduce both the amplitude and connectivity of resting-state BOLD fluctuations (Rack-Gomer et al., 2009; Wong et al., 2012). Caffeine is a widely used stimulant that affects both the neural and vascular systems of the brain through its antagonism of adenosine receptors (Fredholm et al., 1999; Pelligrino et al., 2010). The administration of caffeine significantly reduces cerebral blood flow (Wong et al., 2012) and there is some evidence that it also increases baseline oxygen metabolism (Griffeth et al., 2011). When combined, these changes will tend to decrease baseline blood oxygenation, increasing the parameter M and thus the BOLD response to neural input. However, caffeine also appears to reduce the CBF/CMRO$_2$ coupling ratio n, which would decrease the BOLD signal response to neural activity (Chen and Parrish, 2009; Griffeth et al., 2011). These two opposing effects have been found to result in either no change or a slight increase in the BOLD response to stimulus (Chen and Parrish, 2009; Griffeth et al., 2011; Laurienti et al., 2002; Liau et al., 2008; Mulderink et al., 2002). By taking into account the prior results within the framework of the BOLD signal model, we could conclude that it seems unlikely that caffeine's effects on baseline CBF, CMRO$_2$, and the coupling between CBF and CMRO$_2$ would lead to a decrease in the amplitude of the resting-state BOLD signal.

Hypercapnia has also been shown to reduce the amplitude of resting-state BOLD signals (Biswal et al., 1997; Xu et al., 2011). It is well known that hypercapnia increases CBF, and it is generally assumed that mild hypercapnic stimuli have a minimal effect on neural activity and oxygen metabolism (Chen and Pike, 2010; Jain et al., 2011), although there is some evidence that hypercapnia may decrease CMRO$_2$ (Xu et al., 2011). Both factors (e.g. CBF increase and no change or a slight decrease in CMRO$_2$) will tend to increase baseline venous oxygenation, as has been confirmed through MRI oximetry (Xu et al., 2011). The increased oxygenation will in turn decrease the M factor and reduce the BOLD response. In addition, elevations in baseline CBF tend to reduce the amplitude of CBF responses (Liau and Liu, 2009), resulting in smaller percent BOLD fluctuations. Thus, to first order, the decreases in resting-state BOLD amplitude can be explained by hypercapnia's effect on the baseline vascular state.

Application of normalization and calibration methods to rsfMRI amplitude measures

In addition to using the BOLD signal model to determine how various neurovascular factors modulate the resting-state amplitude, we can adapt the normalization and calibration methods that were originally developed for task-related fMRI, such as division of the resting-state BOLD time courses by the BOLD response to a hypercapnic stimulus. When normalization methods are used, the resulting amplitude estimates will be a scaled version of the original estimates, where the scaling factor varies across subjects and conditions to account for differences in baseline neurovascular states. In the case of the calibrated fMRI approach, the resulting metric of interest (CMRO$_2$ amplitude) is fundamentally different than the original metric (BOLD amplitude), but the overall effect on amplitude estimates can still be viewed as a scaling operation.

As an example of the application of a normalization approach, Xu et al. (2011) normalized the resting-state BOLD amplitudes in the default mode network by the task-related BOLD responses in the visual cortex to more fully probe the effects of hypercapnia. Given that

prior work Zappe et al. (2008) had indicated that hypercapnia had a minimal effect on visual evoked EEG responses, any decrease in the visual evoked fMRI response was treated as a vascular effect. If hypercapnia led to the same percentage decrease in the visual and resting-state amplitudes, then the normalization process would result in identical values for the pre and post-hypercapnia normalized resting state amplitudes, indicating that the decrease in the resting state was completely accounted for by vascular effects. Xu and colleagues found a decrease in the normalized amplitudes (i.e. the relative decrease in resting-state amplitudes was greater than the relative decrease in the visual responses) and interpreted this as evidence for a neuronal component to the reduction in resting-state activity. The specific interpretation is somewhat mitigated by the fact that the authors' specific definition of resting-state amplitude depended on both the amplitude of the fluctuations and the correlation between the seed region and the voxels of interest, thus leading to a possible overestimation of the decrease in resting-state amplitude. In addition, the normalization of the responses in one brain region (e.g. the medial prefrontal cortex) by the task-related responses in another region (visual cortex) may be confounded by inter-regional differences in vascularity (Hendrikse et al., 2010; Mark and Pike, 2012). Nonetheless, the use of task-related responses as a normalization factor represents a promising approach for distinguishing between neural and vascular effects in the resting state and warrants further study.

As noted in a previous section, resting-state measures have also been proposed for the normalization of task-related responses (Biswal et al., 2007; Kannurpatti and Biswal, 2008). The implicit assumption when using either a resting-state measure or task-related response as the normalization reference is that variations in the reference quantity are a reflection of factors (e.g. vascular differences) that also affect the quantity of interest (i.e. the task-related response or resting-state amplitude, respectively), but are not directly related to neural activity. Thus, normalizing by the reference quantity removes the influence of a common non-neural factor. However, as discussed in further detail in Liu et al. (2013), there is growing evidence in support of a significant neural contribution to variations in measures (e.g. task-related BOLD responses, hypercapnic BOLD responses, resting-state BOLD activity, baseline cerebral blood flow) that have been used for normalization approaches. As a result, normalization methods that use these measures to remove variability in the either resting-state or task-related BOLD measures run the risk of removing differences that are of neural origin. Further work is needed to better understand these confounds. In the mean time, it would be prudent for researchers to take into account this potential effect when normalizing their BOLD fMRI data.

Interpreting changes in resting-state connectivity

There are a number of ways in which neurovascular factors can alter measures of connectivity: (1) reducing the amplitude of the fluctuations of interest relative to the amplitude of nuisance signals; (2) changing the relative shape of the hemodynamic response; and (3) changing the relative delay of the hemodynamic response. To better understand these effects, we consider a simplified model (depicted in Fig. 1) in which the measured responses from two brain regions are denoted as: $x_1(t) = s_1(t) + n_1(t)$ and $x_2(t) = s_2(t) + n_2(t)$, where $s_i(t)$ and $n_i(t)$ represent the signal of interest and noise signal (including both random and structured noise) in the ith brain region, respectively, and it is assumed that the signal is uncorrelated with the noise signals and that the variance of the signal (or noise) terms is independent of region (i.e. $\sigma_{s_1}^2 = \sigma_{s_2}^2 = \sigma_s^2$ and $\sigma_{n_1}^2 = \sigma_{n_2}^2 = \sigma_n^2$) With these simplifying assumptions, the correlation coefficient may be written in the following form:

$$r = r_s \left(\frac{\mathrm{SNR} + r_n/r_s}{\mathrm{SNR} + 1} \right) \quad (2)$$

where $r_s = \mathrm{corr}(s_1, s_2)$ is the correlation between the signal terms, $r_n = \mathrm{corr}(n_1, n_2)$ is the correlation between the noise terms, $\mathrm{SNR} = \sigma_s^2/\sigma_n^2$ denotes the signal-to-noise-ratio, and σ_s^2 and σ_n^2 are the signal and noise variances, respectively (see Appendix A for derivation). The form of Eq. (2) enables us to distinguish between effects that alter SNR versus those that alter the correlation between signal terms.

Changes in connectivity measures due to decreases in BOLD signal amplitude

The simplest case to consider is one in which a neurovascular factor reduces the amplitude of the signals of interest while not affecting either the amplitude of the noise terms or the correlation r_s between the signal terms of interest. For example, this could be a factor such as hypercapnia that reduces the M parameter in the BOLD signal model for the response to neural fluctuations but does not alter the amplitude of structured noise signals due to cardiac fluctuations or motion. The main effect of this factor is to reduce the SNR term. From the form of Eq. (2), the measured correlation tends towards the signal correlation value r_s as the SNR increases, but approaches the noise correlation value r_n as the SNR decreases. For the case that $r_s > r_n$, a SNR decrease will reduce the measured correlation value r as shown by the green dashed line in Fig. 3A, which shows the dependence of r on SNR when it is assumed that $r_s = 0.5$ and $r_n = 0.3$. The blue solid line in Fig. 3A shows the dependence on SNR when $r_n = 0.7$ is greater than the assumed $r_s = 0.5$—here decreases in SNR can lead to an increase in the measured correlation as the noise term dominates. For long-range functional connections, where it is likely that signal correlations will be greater than noise correlations, it is expected that $r_s > r_n$ and so SNR decreases will in general lead to reductions in the measured correlation. For example, the connectivity decreases observed with hypercapnia (Biswal et al., 1997; Xu et al., 2011) could be viewed as reflecting the SNR decrease caused by a neurovascular reduction in the amplitude of the BOLD signal fluctuations of interest. Fig. 1 provides a schematic description of this effect. In this figure, the measured BOLD signals are calculated under two conditions: (1) full amplitude hemodynamic responses, indicated by the blue and red responses and (2) reduced amplitude (scaled by 0.33) hemodynamic responses, indicated by the black and green responses. For the full amplitude responses, the signal and noise correlations are $r_s = 0.70$ and $r_n = 0.38$, respectively, the SNR is equal to 1.0, and the measured correlation is 0.54. For the reduced amplitude responses, the signal and noise correlations remain unchanged, but the SNR drops to 0.33 and the measured correlation decreases to 0.41. This decrease is consistent with the theoretical predictions as shown by the red square and black diamond symbols for the full and reduced amplitude responses, respectively, in Fig. 3B.

Changes in connectivity measures due to alteration of the hemodynamic response

Neurovascular factors that alter the shape of the hemodynamic response can affect both the signal variance term σ_s^2 and the signal correlation term r_s. Because the measured BOLD fluctuations can be viewed as the convolution of the underlying neural power fluctuations convolved with the hemodynamic response (de Munck et al., 2007), a significant change in the temporal shape (or equivalently the frequency response) of the response can affect the amplitude of the fluctuations. For example, a temporal broadening of the response would

result in a smaller passband in the frequency domain, leading to an attenuation of higher frequency fluctuations. A reduction in signal amplitude due to a change in the response shape can decrease the measured correlation r through reducing the SNR, as discussed previously. In addition, inter-regional differences in the response shape can affect the measured correlation through modulation of the signal correlation term r_s. For example, if a pharmacological factor, such as alcohol (Luchtmann et al., 2010), significantly alters the temporal width or delay of the response in one region but not another, this will alter the temporal relationship between the signals more than if both responses had been similarly altered. A schematic representation of these types of effects is shown in Fig. 4. A slowing down of the hemodynamic responses (shown as the black and green responses) in both brain regions, results in a decrease in the correlation between the measured BOLD responses. An even greater decrease in correlation occurs when the response in region 1 remains unchanged (blue response) while the response in region 2 (green response) slows down.

To assess the effect of hemodynamic shape changes on connectivity, one can use either prior knowledge of the changes, such as prior work measuring and modeling the effect of hypercapnia on the shape of the BOLD response (Behzadi and Liu, 2005; Cohen et al., 2002) or obtain estimates of the hemodynamic response under varying conditions, similar to approaches developed for task-related fMRI (Handwerker et al., 2004). Using the expected changes in shape, an investigator could use simulations to model their effect on connectivity measures. For example, the resting-state data from one condition could be further filtered to reflect an additional broadening in the hemodynamic response in another condition and the resulting effects on connectivity could be assessed. One of the key challenges in implementing this type of approach is the difficulty and added experimental complexity in obtaining reliable estimates of the hemodynamic responses. While it is straight forward to obtain these estimates in the visual and motor areas, it is considerably more challenging to obtain such estimates over the entire brain. The use of a breath holding task (which induces hypercapnia) has been presented as a means to obtain estimate of variations in the hemodynamic delays across the brain (Chang et al., 2008), but it is not clear whether the delays in response to a hypercapnic stimulus are the same as those in response to neural activity.

In addition to complexities described above, it is expected that in general the overall effects of changes in the shape of the hemodynamic response will be small due to the significant amount of lowpass filtering that is common in most rsfMRI studies. For example, the temporal shifts caused by hypercapnia are on the order of 1 to 2 s, whereas the time constant of the low-pass filtering operation is typically on the order of 10 s. With this difference in temporal scales, the lowpass filtering operation will tend to blur out the dynamic changes due to hypercapnia. An important caveat is that with advances in acquisition and analysis methods (Feinberg et al., 2010), there is a trend towards acquiring resting data with higher temporal resolution (e.g. whole brain coverage in less than 1 s) and less aggressive filtering. With these emerging methods, the effect of changes in the temporal response dynamics may become more pronounced.

Other approaches for interpreting connectivity changes

In addition to specific arguments based on SNR or changes in the shape of the hemodynamic response, more general arguments have been used to assess the potential effect of neurovascular factors on connectivity. For example, Boveroux et al. (2010) argued that propofol induced decreases in frontoparietal network connectivity were unlikely to reflect the hemodynamic effects of the anesthetic as prior studies had shown that propofol at sedative concentrations did not modulate either the magnitude of the CBF response to stimulus or the coupling of flow and metabolism (Johnston et al., 2003; Veselis et al., 2005).

In addition, because connectivity was preserved in auditory and visual networks, the authors concluded that it was unlikely that their findings were due to either a global reduction in SNR or a global alteration in neurovascular coupling. In a similar study, Stamatakis et al. (2010) found that propofol increased the connectivity of the posterior cingulate cortex with brain regions, such as the motor cortex, that are not typically considered part of the default mode network. While also citing the prior work of Johnston et al. (2003), and Veselis et al. (2005) as evidence against a neurovascular explanation for the effects, the authors further argued that the propofol-induced shift in the predominant temporal frequencies of the resting-state fluctuations were unlikely to have a vascular origin.

Applying normalization and calibration methods to connectivity estimates

The normalization and calibration methods that were discussed above for the resting-state amplitude estimates can also be applied to estimates of connectivity, but the effects are not as straightforward. Normalization methods will primarily lead to a scaling of the measured time courses, and this scaling will not alter the correlation estimate, as the correlation coefficient is invariant with respect to amplitude scaling. On the other hand, for calibration approaches that combine CBF and BOLD time courses to form an estimate of the $CMRO_2$ time courses, the correlation between the $CMRO_2$ time courses can be significantly different than the correlation between the BOLD time courses. For example, the resting-state $CMRO_2$ fluctuations estimated in Wu et al. (2009) were essentially scaled versions of the CBF fluctuations, due to the relatively small amplitude of the BOLD fluctuations as compared to the parameter M (Restom et al., 2008). As a result, the $CMRO_2$ correlation maps were similar to the CBF maps but were qualitatively different from the BOLD correlation maps. It should also be noted that the validity of applying the calibrated fMRI approach to resting-state fMRI data has not yet been fully established. Because the Davis approach assumes a causal dependence of BOLD on CBF, the effective estimation of the $CMRO_2$ response requires that both the BOLD and CBF responses are measured with sufficient sensitivity such that a relation between the two quantities can be firmly established. While there is typically a strong correlation between the BOLD and CBF responses for task-related paradigms (especially for strong sensory stimuli), this is not necessarily the case for resting-state data in which the correlation between the BOLD and CBF time courses can be quite low (Wu et al., 2009), due primarily to the low inherent sensitivity of the arterial spin labeling MRI method that is used to estimate CBF (Liu and Brown, 2007). The sensitivity of the resting state CBF measures can be improved with the use of background suppression methods, such as those as used in Fukunaga et al. (2008), but the quantitative accuracy of CBF measures obtained with these methods is still an area of active investigation (Garcia et al., 2005; Shin et al., 2011).

Global signal regression and physiological noise correction

One of the methodological issues that complicates the interpretation of resting-state studies is the inconsistent use of global signal regression (GSR) in the pre-processing of the data. GSR refers to the removal of a global mean signal component (computed as the average of all the BOLD time series in the brain) prior to the computation of the correlation coefficients. This step has been shown to be beneficial for improving the predictive power of correlation measures (Fox et al., 2009). When global signal regression is not used, a strong global component often dominates the computation of the correlation coefficients, leading to significant variations between functional connectivity maps acquired from different experimental scans or subjects. The validity of global signal regression has recently come under question because the mathematics of the regression process causes the distribution of correlation coefficients to be centered about zero, thereby forcing the existence of negative correlations (Murphy et al., 2009; Weissenbacher et al., 2009). In particular, Murphy et al.

(2009) argued that the anti-correlations between the default mode network (DMN) and the task positive network (TPN) reported by Fox et al. (2005) were an artifact of global signal regression.

To circumvent the potential issues with global signal regression, alternate methods have been developed to remove global signal components that are of physiological origin (i.e. due to either respiratory or cardiac activity). These include (1) the use of mean signals from white matter and cerebral spinal fluid regions to estimate the physiological components and (2) the formation of regressors from external measures of cardiac and respiratory activity (Birn et al., 2006; Chang and Glover, 2009; Fox et al., 2009). However, at present, there is not a clear consensus with regards to the best approach for addressing global signal confounds, with many studies still continuing to use global signal regression, while a growing number of studies have begun to adopt one of the alternate methods (Chai et al., 2012). This lack of agreement makes it difficult to compare resting-state fMRI studies, as differing approaches can yield significantly different interpretations of the data. For example, in their study of the effects of caffeine on resting-state connectivity, Wong et al. (2012) compared functional connectivity maps obtained using GSR with maps obtained using only physiological regressors (motion, cardiac and respiratory activity, white matter and cerebral spinal fluid signals). They found that the effects of caffeine were greatly diminished with the application of GSR, with strong anti-correlations between the DMN and TPN observed both prior to and after the administration of caffeine. In contrast, when only physiological regressors were used, the anti-correlations between the two networks were only weakly visible in the pre-dose state but significantly enhanced after the intake of caffeine. In interpreting their findings, Wong et al. concluded that the main effect of caffeine was consistent with the reduction of an additive global signal component (He and Liu, 2012), most likely of neural origin. Since GSR had already eliminated this additive component in the pre-dose state, it masked caffeine's attenuation of this component in the post-dose state. Until the controversy about the validity of GSR is settled, it would be prudent for most investigators to analyze their data with and without the application of GSR, especially when interpreting studies in which neurovascular factors may affect the global signal component. An alternative approach is to compare connectivity results based on correlation analysis and GSR with those obtained using an independent components analysis approach (Boveroux et al., 2010).

In addition to GSR, the application of other physiological noise correction methods has been shown to affect estimates of BOLD signal variance and resting-state connectivity (Khalili-Mahani et al., 2013). This problem can be especially pronounced for studies in which the physiological noise regressors are themselves modulated by the experimental factor, such as the modulation of respiration and heart rate by morphine. In a detailed study of the effect of various physiological noise correction approaches, Khalili-Mahani et al. (2013) reported greater sensitivity in brain regions that were either close to large vessels or involved in physiological regulation, such as the posterior cingulate cortex, and found that the effects were greatest when including physiological rates in higher level statistical analyses.

EEG and MEG measures of resting-state activity

While the use of the BOLD signal model and associated normalization and calibration approaches provides an important starting point for assessing the effect of neurovascular factors on resting-state amplitudes and connectivity, the ability to definitively determine relative changes in neural and vascular components of resting state activity is limited when only fMRI measures are available. For example, while arguments based on the BOLD signal model suggest that the reduction in resting-state BOLD amplitude due to hypercapnia is consistent with an increase in the baseline deoxyhemoglobin content, there still remains the

possibility that the amplitude reduction might also reflect a decrease in the underlying neural power fluctuations. The acquisition of additional electroencephalographic (EEG) or magnetoencephalographic (MEG) measures can be employed to address this ambiguity. Non-invasive simultaneous EEG/fMRI recordings in humans have shown that resting-state BOLD fluctuations are significantly correlated with fluctuations in the power of EEG activity in the alpha band (de Munck et al., 2007; Goldman et al., 2002; Laufs et al., 2003a; Moosmann et al., 2003; Ritter et al., 2008), the beta band (Laufs et al., 2003b), and the theta band (Scheeringa et al., 2008). Using independent component analysis, Mantini et al. (2007) found that the BOLD time courses associated with various resting-state networks (identified as independent components) exhibited strong correlations with the power in more than one EEG band. A number of studies have focused on examining the inter-regional connectivity between MEG resting-state power fluctuations and have demonstrated a striking similarity between MEG and fMRI resting-state networks (Brookes et al., 2011a, 2011b; de Pasquale et al., 2010; Liu et al., 2010; Mantini et al., 2011).

With respect to the effects of hypercapnia on resting-state activity, Xu et al. (2011) found EEG power decreases in the alpha band and increases in the delta band, while Hall et al. (2011) found MEG power decreases in the alpha, beta, and low gamma bands. Given the relation between resting-state alpha power and BOLD fluctuations, these observations suggest that the decrease in resting-state BOLD amplitude is not just due to a reduction in baseline deoxyhemoglobin but may also reflect an attenuation of the neural power fluctuations.

Boly et al. (2012) used source localized EEG and dynamic causal modeling (Kiebel et al., 2009) to demonstrate the effect of the anesthesia propofol on corticocortical backward connectivity and thalamocortical connectivity in the EEG measures. These findings extended the group's prior findings of a decrease in cerebral resting state BOLD connectivity, which the previous study had included were unlikely to reflect vascular effects, as discussed in a previous section (Boveroux et al., 2010).

In considering the effects of caffeine, we noted in a previous section that it was unlikely that baseline vascular and metabolic changes could cause the observed decrease in resting-state BOLD amplitude, suggesting instead a reduction in the level of neural power fluctuations. Indeed EEG studies have demonstrated a decrease in alpha power due to caffeine (Barry et al., 2008; Siepmann and Kirch, 2002). In a recent simultaneous EEG-fMRI study, Wong et al. (2013) focusedon the shape of the EEG power spectra and founda caffeine-induced shift from lower (delta and theta) frequency bands to higher (alpha) bands, consistent with a transition to higher levels of vigilance (Horovitz et al., 2008; Klimesch, 1999; Olbrich et al., 2009). In addition, increases in the EEG measures of vigilance (defined as the ratio of the power in the alpha band to the power in the delta and theta bands (Horovitz et al., 2008)) were shown to be related to decreases in the resting-state BOLD global signal amplitude. Furthermore, using the MEG beamformer analysis approach developed by Brookes et al. (2011a, 2011b), Tal et al. (2013) found that fMRI and MEG measures of connectivity exhibited similar decreases across the entire brain. Overall, the EEG and MEG measures provide strong evidence that the caffeine-related decreases in both resting-state amplitude and connectivity reflect changes in the neural power fluctuations.

Conclusion

While there is a growing appreciation for the role of neurovascular factors in rsfMRI, the development of approaches to address neurovascular confounds is still in its infancy. Methods developed to deal with these confounds in task-related fMRI can serve as a useful starting point, but the validity and accuracy of these methods are still an active area of

investigation even for task-related studies, and not all of the methods are applicable to rsfMRI. In addition, the analysis and interpretation challenges are greater in rsfMRI because the temporal evolution of the resting-state BOLD signal is not determined by an external stimulus. As a result, the continued application of multimodal approaches, such as simultaneous EEG-fMRI, will be critical for furthering our understanding of the relative contribution of neural and vascular factors to rsfMRI measures. In this paper, we have focused on pharmacological modulations of the neurovascular state, where the ability to modulate the state in a controlled fashion facilitates the design and interpretation of the studies. However, there is a great need for additional studies that can help to further our understanding of disease-related factors. Improvements in our ability to address neurovascular confounds will be especially critical for the robust application of rsfMRI in clinical environments, where alterations in neural activity and neurovascular coupling due to disease, medication, and age are both widespread and diverse.

Acknowledgments

Appendix A. Derivation of Eq. (2)

Let r denote the correlation between $x_1(t) = s_1(t) + n_1(t)$ and $x_2(t) = s_2(t) + n_2(t)$. We assume that the signals $s_i(t)$ are uncorrelated with the noise signals $n_i(t)$, and that the variance of the signal (or noise) terms is independent of region (i.e $\sigma_{s_1}^2 = \sigma_{s_2}^2 = \sigma_s^2$ and $\sigma_{n_1}^2 = \sigma_{n_2}^2 = \sigma_n^2$). Then the correlation may be written as:

$$
\begin{aligned}
r &= \frac{\text{cov}(s_1+n_1, s_2+n_2)}{\text{std}(s_1+n_1)\,\text{std}(s_2+n_2)} \\
&= \frac{\text{cov}(s_1, s_2) + \text{cov}(n_1, n_2)}{\sqrt{\sigma_{s_1}^2+\sigma_{n_1}^2}\,\sqrt{\sigma_{s_2}^2+\sigma_{n_2}^2}} \\
&= \frac{\text{cov}(s_1, s_2) + \text{cov}(n_1, n_2)}{\sigma_s^2 + \sigma_n^2} \\
&= \frac{\frac{\text{cov}(s_1,s_2)}{\sigma_s^2}\frac{\sigma_s^2}{\sigma_n^2} + \frac{\text{cov}(n_1,n_2)}{\sigma_n^2}}{\sigma_s^2/\sigma_n^2 + 1} \\
&= \frac{r_s \text{SNR} + r_n}{\text{SNR}+1} \\
&= r_s\left(\frac{\text{SNR}+r_n/r_s}{\text{SNR}+1}\right)
\end{aligned}
$$

where $r_s = \text{corr}(s_1,s_2)$ is the correlation between the signal terms, $r_n = \text{corr}(n_1,n_2)$ is the correlation between the noise terms, and $\text{SNR}=\sigma_s^2/\sigma_n^2$ denotes the signal-to-noise-ratio.

References

Allen G, Barnard H, McColl R, Hester AL, Fields JA, Weiner MF, Ringe WK, Lipton AM, Brooker M, McDonald E, Rubin CD, Cullum CM. Reduced hippocampal functional connectivity in Alzheimer disease. Arch Neurol. 2007; 64:1482–1487. [PubMed: 17923631]

Barry RJ, Clarke AR, Johnstone SJ, Rushby JA. Timing of caffeine's impact on autonomic and central nervous system measures: clarification of arousal effects. Biol Psychol. 2008; 77:304–316. [PubMed: 18093716]

Behzadi Y, Liu TT. An arteriolar compliance model of the cerebral blood flow response to neural stimulus. Neuroimage. 2005; 25:1100–1111. [PubMed: 15850728]

Birn RM, Diamond JB, Smith MA, Bandettini PA. Separating respiratory- variation-related fluctuations from neuronal-activity-related fluctuations in fMRI. Neuroimage. 2006; 31:1536–1548. [PubMed: 16632379]

Biswal B, Hudetz AG, Yetkin FZ, Haughton VM, Hyde JS. Hypercapnia reversibly suppresses low-frequency fluctuations in the human motor cortex during rest using echo-planar MRI. J Cereb Blood Flow Metab. 1997; 17:301–308. [PubMed: 9119903]

Biswal BB, Kannurpatti SS, Rypma B. Hemodynamic scaling of fMRI-BOLD signal: validation of low-frequency spectral amplitude as a scalability factor. Magn Reson Imaging. 2007; 25:1358–1369. [PubMed: 17482411]

Boly M, Moran R, Murphy M, Boveroux P, Bruno MA, Noirhomme Q, Ledoux D, Bonhomme V, Brichant JF, Tononi G, Laureys S, Friston K. Connectivity changes underlying spectral EEG changes during propofol-induced loss of consciousness. J Neurosci. 2012; 32:7082–7090. [PubMed: 22593076]

Boveroux P, Vanhaudenhuyse A, Bruno MA, Noirhomme Q, Lauwick S, Luxen A, Degueldre C, Plenevaux A, Schnakers C, Phillips C, Brichant JF, Bonhomme V, Maquet P, Greicius MD, Laureys S, Boly M. Breakdown of within- and between-network resting state functional magnetic resonance imaging connectivity during propofol-induced loss of consciousness. Anesthesiology. 2010; 113:1038–1053. [PubMed: 20885292]

Brookes MJ, Hale JR, Zumer JM, Stevenson CM, Francis ST, Barnes GR, Owen JP, Morris PG, Nagarajan SS. Measuring functional connectivity using MEG: methodology and comparison with fcMRI. Neuroimage. 2011a; 56:1082–1104. [PubMed: 21352925]

Brookes MJ, Woolrich M, Luckhoo H, Price D, Hale JR, Stephenson MC, Barnes GR, Smith SM, Morris PG. Investigating the electrophysiological basis of resting state networks using magnetoencephalography. Proc Natl Acad Sci U S A. 2011b; 108:16783–16788. [PubMed: 21930901]

Buxton RB, Uludag K, Dubowitz DJ, Liu TT. Modeling the hemodynamic response to brain activation. Neuroimage. 2004; 23(Suppl. 1):S220–S233. [PubMed: 15501093]

Carusone LM, Srinivasan J, Gitelman DR, Mesulam MM, Parrish TB. Hemodynamic response changes in cerebrovascular disease: implications for functional MR imaging. AJNR Am J Neuroradiol. 2002; 23:1222–1228. [PubMed: 12169483]

Chai XJ, Castañón AN, Ongür D, Whitfield-Gabrieli S. Anticorrelations in resting state networks without global signal regression. Neuroimage. 2012; 59:1420–1428. [PubMed: 21889994]

Chang C, Glover GH. Effects of model-based physiological noise correction on default mode network anti-correlations and correlations. Neuroimage. 2009; 47:1448–1459. [PubMed: 19446646]

Chang C, Thomason ME, Glover GH. Mapping and correction of vascular hemodynamic latency in the BOLD signal. Neuroimage. 2008; 43:90–102. [PubMed: 18656545]

Chen Y, Parrish TB. Caffeine's effects on cerebrovascular reactivity and coupling between cerebral blood flow and oxygen metabolism. Neuroimage. 2009; 44:647–652. [PubMed: 19000770]

Chen JJ, Pike GB. Global cerebral oxidative metabolism during hypercapnia and hypocapnia in humans: implications for BOLD fMRI. J Cereb Blood Flow Metab. 2010; 30:1094–1099. [PubMed: 20372169]

Chiarelli PA, Bulte DP, Wise R, Gallichan D, Jezzard P. A calibration method for quantitative BOLD fMRI based on hyperoxia. Neuroimage. 2007; 37:808–820. [PubMed: 17632016]

Cohen ER, Ugurbil K, Kim SG. Effect of basal conditions on the magnitude and dynamics of the blood oxygenation level-dependent fMRI response. J Cereb Blood Flow Metab. 2002; 22:1042–1053. [PubMed: 12218410]

Cohen ER, Rostrup E, Sidaros K, Lund TE, Paulson OB, Ugurbil K, Kim SG. Hypercapnic normalization of BOLD fMRI: comparison across field strengths and pulse sequences. Neuroimage. 2004; 23:613–624. [PubMed: 15488411]

Davis TL, Kwong KK, Weisskoff RM, Rosen BR. Calibrated functional MRI: mapping the dynamics of oxidative metabolism. Proc Natl Acad Sci U S A. 1998; 95:1834–1839. [PubMed: 9465103]

de Munck JC, Goncalves SI, Huijboom L, Kuijer JP, Pouwels PJ, Heethaar RM, Lopes da Silva FH. The hemodynamic response of the alpha rhythm: an EEG/fMRI study. Neuroimage. 2007; 35:1142–1151. [PubMed: 17336548]

de Pasquale F, Della Penna S, Snyder AZ, Lewis C, Mantini D, Marzetti L, Belardinelli P, Ciancetta L, Pizzella V, Romani GL, Corbetta M. Temporal dynamics of spontaneous MEG activity in brain networks. Proc Natl Acad Sci U S A. 2010; 107:6040–6045. [PubMed: 20304792]

D'Esposito M, Deouell LY, Gazzaley A. Alterations in the BOLD fMRI signal with ageing and disease: a challenge for neuroimaging. Nat Rev Neurosci. 2003; 4:863–872. [PubMed: 14595398]

Feinberg DA, Moeller S, Smith SM, Auerbach E, Ramanna S, Glasser MF, Miller KL, Ugurbil K, Yacoub E. Multiplexed echo planar imaging for subsecond whole brain FMRI and fast diffusion imaging. PLoS One. 2010; 5:e15710. [PubMed: 21187930]

Fox MD, Raichle ME. Spontaneous fluctuations in brain activity observed with functional magnetic resonance imaging. Nat Rev Neurosci. 2007; 8:700–711. [PubMed: 17704812]

Fox MD, Snyder AZ, Vincent JL, Corbetta M, Van Essen DC, Raichle ME. The human brain is intrinsically organized into dynamic, anticorrelated functional networks. Proc Natl Acad Sci U S A. 2005; 102:9673–9678. [PubMed: 15976020]

Fox MD, Zhang D, Snyder AZ, Raichle ME. The global signal and observed anticorrelated resting state brain networks. J Neurophysiol. 2009; 101:3270–3283. [PubMed: 19339462]

Fredholm BB, Battig K, Holmen J, Nehlig A, Zvartau EE. Actions of caffeine in the brain with special reference to factors that contribute to its widespread use. Pharmacol Rev. 1999; 51:83–133. [PubMed: 10049999]

Fukunaga M, Horovitz S, De Zwart J, Van Gelderen P, Balkin T, Braun A, Duyn J. Metabolic origin of BOLD signal fluctuations in the absence of stimuli. J Cereb Blood Flow Metab. 2008; 28:1377–1387. [PubMed: 18382468]

Garcia DM, Duhamel G, Alsop DC. Efficiency of inversion pulses for background suppressed arterial spin labeling. Magn Reson Med. 2005; 54:366–372. [PubMed: 16032674]

Gauthier CJ, Hoge RD. Magnetic resonance imaging of resting OEF and CMRO using a generalized calibration model for hypercapnia and hyperoxia. Neuroimage. 2012; 60:1212–1225. [PubMed: 22227047]

Gauthier CJ, Desjardins-Crépeau L, Madjar C, Bherer L, Hoge RD. Absolute quantification of resting oxygen metabolism and metabolic reactivity during functional activation using QUO_2 MRI. Neuroimage. 2012; 63:1353–1363. [PubMed: 22986357]

Goldman RI, Stern JM, Engel J Jr, Cohen MS. Simultaneous EEG and fMRI of the alpha rhythm. Neuroreport. 2002; 13:2487–2492. [PubMed: 12499854]

Greicius MD, Srivastava G, Reiss AL, Menon V. Default-mode network activity distinguishes Alzheimer's disease from healthy aging: evidence from functional MRI. Proc Natl Acad Sci U S A. 2004; 101:4637–4642. [PubMed: 15070770]

Greicius MD, Kiviniemi V, Tervonen O, Vainionpaa V, Alahuhta S, Reiss AL, Menon V. Persistent default-mode network connectivity during light sedation. Hum Brain Mapp. 2008; 29:839–847. [PubMed: 18219620]

Griffeth VEM, Perthen JE, Buxton RB. Prospects for quantitative fMRI: investigating the effects of caffeine on baseline oxygen metabolism and the response to a visual stimulus in humans. Neuroimage. 2011; 57:809–816. [PubMed: 21586328]

Hall EL, Driver ID, Croal PL, Francis ST, Gowland PA, Morris PG, Brookes MJ. The effect of hypercapnia on resting and stimulus induced MEG signals. Neuroimage. 2011; 58:1034–1043. [PubMed: 21762783]

Handwerker DA, Ollinger JM, D'Esposito M. Variation of BOLD hemodynamic responses across subjects and brain regions and their effects on statistical analyses. Neuroimage. 2004; 21:1639–1651. [PubMed: 15050587]

Handwerker DA, Gazzaley A, Inglis BA, D'esposito M. Reducing vascular variability of fMRI data across aging populations using a breathholding task. Hum Brain Mapp. 2007; 28:846–859. [PubMed: 17094119]

He H, Liu TT. A geometric view of global signal confounds in resting-state functional MRI. Neuroimage. 2012; 59:2339–2348. [PubMed: 21982929]

He Y, Wang L, Zang Y, Tian L, Zhang X, Li K, Jiang T. Regional coherence changes in the early stages of Alzheimer's disease: a combined structural and resting-state functional MRI study. Neuroimage. 2007; 35:488–500. [PubMed: 17254803]

Hendrikse J, Petersen ET, Chng SM, Venketasubramanian N, Golay X. Distribution of cerebral blood flow in the nucleus caudatus, nucleus lentiformis, and thalamus: a study of territorial arterial spin-labeling MR imaging. Radiology. 2010; 254:867–875. [PubMed: 20089720]

Hoge RD, Atkinson J, Gill B, Crelier GR, Marrett S, Pike GB. Investigation of BOLD signal dependence on cerebral blood flow and oxygen consumption: the deoxyhemoglobin dilution model. Magn Reson Med. 1999a; 42:849–863. [PubMed: 10542343]

Hoge RD, Atkinson J, Gill B, Crelier GR, Marrett S, Pike GB. Linear coupling between cerebral blood flow and oxygen consumption in activated human cortex. Proc Natl Acad Sci U S A. 1999b; 96:9403–9408. [PubMed: 10430955]

Horovitz SG, Fukunaga M, De Zwart JA, Van Gelderen P, Fulton SC, Balkin TJ, Duyn JH. Low frequency BOLD fluctuations during resting wakefulness and light sleep: a simultaneous EEG-fMRI study. Hum Brain Mapp. 2008; 29:671–682. [PubMed: 17598166]

Iadecola C. Neurovascular regulation in the normal brain and in Alzheimers disease. Nat Rev Neurosci. 2004; 5:347–360. [PubMed: 15100718]

Iannetti G, Wise R. BOLD functional MRI in disease and pharmacological studies: room for improvement? Magn Reson Imaging. 2007; 25:978–988. [PubMed: 17499469]

Jain V, Langham MC, Floyd TF, Jain G, Magland JF, Wehrli FW. Rapid magnetic resonance measurement of global cerebral metabolic rate of oxygen consumption in humans during rest and hypercapnia. J Cereb Blood Flow Metab. 2011; 31:1504–1512. [PubMed: 21505481]

Johnston AJ, Steiner LA, Chatfield DA, Coleman MR, Coles JP, Al-Rawi PG, Menon DK, Gupta AK. Effects of propofol on cerebral oxygenation and metabolism after head injury. Br J Anaesth. 2003; 91:781–786. [PubMed: 14633744]

Kannurpatti SS, Biswal BB. Detection and scaling of task-induced fMRI-BOLD response using resting state fluctuations. Neuroimage. 2008; 40:1567–1574. [PubMed: 18343159]

Khalili-Mahani N, Zoethout RMW, Beckmann CF, Baerends E, de Kam ML, Soeter RP, Dahan A, van Buchem MA, van Gerven JMA, Rombouts SARB. Effects of morphine and alcohol on functional brain connectivity during "resting state": a placebo-controlled crossover study in healthy young men. Hum Brain Mapp. 2012; 33:1003–1018. [PubMed: 21391283]

Khalili-Mahani N, Chang C, van Osch MJ, Veer IM, van Buchem MA, Dahan A, Beckmann CF, van Gerven JMA, Rombouts SARB. The impact of "physiological correction" on functional connectivity analysis of pharmacological resting state fMRI. Neuroimage. 2013; 65:499–510. [PubMed: 23022093]

Kiebel SJ, Garrido MI, Moran R, Chen CC, Friston KJ. Dynamic causal modeling for EEG and MEG. Hum Brain Mapp. 2009; 30:1866–1876. [PubMed: 19360734]

Kiviniemi VJ, Haanpaa H, Kantola JH, Jauhiainen J, Vainionpaa V, Alahuhta S, Tervonen O. Midazolam sedation increases fluctuation and synchrony of the resting brain BOLD signal. Magn Reson Imaging. 2005; 23:531–537. [PubMed: 15919598]

Klimesch W. EEG alpha and theta oscillations reflect cognitive and memory performance: a review and analysis. Brain Res Brain Res Rev. 1999; 29:169–195. [PubMed: 10209231]

Laufs H, Kleinschmidt A, Beyerle A, Eger E, Salek-Haddadi A, Preibisch C, Krakow K. EEG-correlated fMRI of human alpha activity. Neuroimage. 2003a; 19:1463–1476. [PubMed: 12948703]

Laufs H, Krakow K, Sterzer P, Eger E, Beyerle A, Salek-Haddadi A, Kleinschmidt A. Electroencephalographic signatures of attentional and cognitive default modes in spontaneous brain activity fluctuations at rest. Proc Natl Acad Sci U S A. 2003b; 100:11053–11058. [PubMed: 12958209]

Laurienti PJ, Field AS, Burdette JH, Maldjian JA, Yen YF, Moody DM. Dietary caffeine consumption modulates fMRI measures. Neuroimage. 2002; 17:751–757. [PubMed: 12377150]

Li SJ, Biswal B, Li Z, Risinger R, Rainey C, Cho JK, Salmeron BJ, Stein EA. Cocaine administration decreases functional connectivity in human primary visual and motor cortex as detected by functional MRI. Magn Reson Med. 2000; 43:45–51. [PubMed: 10642730]

Li SJ, Li Z, Wu G, Zhang MJ, Franczak M, Antuono PG. Alzheimer disease: evaluation of a functional MR imaging index as a marker. Radiology. 2002; 225:253–259. [PubMed: 12355013]

Liau J, Liu TT. Inter-subject variability in hypercapnic normalization of the BOLD fMRI response. Neuroimage. 2009; 45:420–430. [PubMed: 19111622]

Liau J, Perthen JE, Liu TT. Caffeine reduces the activation extent and contrast-to-noise ratio of the functional cerebral blood flow response but not the BOLD response. Neuroimage. 2008; 42:296–305. [PubMed: 18514545]

Lindauer U, Dirnagl U, Füchtemeier M, Böttiger C, Offenhauser N, Leithner C, Royl G. Pathophysiological interference with neurovascular coupling—when imaging based on hemoglobin might go blind. Front Neuroenergetics. 2010; 2

Liu TT, Brown GG. Measurement of cerebral perfusion with arterial spin labeling: Part 1. Methods J Int Neuropsychol Soc. 2007; 13:517–525.

Liu Y, Wang K, Yu C, He Y, Zhou Y, Liang M, Wang L, Jiang T. Regional homogeneity, functional connectivity and imaging markers of Alzheimer's disease: a review of resting-state fMRI studies. Neuropsychologia. 2008; 46:1648–1656. [PubMed: 18346763]

Liu Z, Fukunaga M, De Zwart JA, Duyn JH. Large-scale spontaneous fluctuations and correlations in brain electrical activity observed with magnetoencephalography. Neuroimage. 2010; 51:102–111. [PubMed: 20123024]

Liu TT, Glover GH, Mueller BA, Greve DN, Brown GG. An introduction to normalization and calibration methods in functional MRI. Psychometrika. 2013; 78:308–321.

Lu H, Yezhuvath US, Xiao G. Improving fMRI sensitivity by normalization of basal physiologic state. Hum Brain Mapp. 2010; 31:80–87. [PubMed: 19585589]

Luchtmann M, Jachau K, Tempelmann C, Bernarding J. Alcohol induced region-dependent alterations of hemodynamic response: implications for the statistical interpretation of pharmacological fMRI studies. Exp Brain Res. 2010; 204:1–10. [PubMed: 20502888]

Maandag NJ, Coman D, Sanganahalli BG, Herman P, Smith AJ, Blumenfeld H, Shulman RG, Hyder F. Energetics of neuronal signaling and fMRI activity. Proc Natl Acad Sci U S A. 2007; 104:20546–20551. [PubMed: 18079290]

Mantini D, Perrucci MG, Del Gratta C, Romani GL, Corbetta M. Electrophysiological signatures of resting state networks in the human brain. Proc Natl Acad Sci U S A. 2007; 104:13170–13175. [PubMed: 17670949]

Mantini D, Della Penna S, Marzetti L, de Pasquale F, Pizzella V, Corbetta M, Romani GL. A signal-processing pipeline for magnetoencephalography resting-state networks. Brain Connect. 2011; 1:49–59. [PubMed: 22432954]

Mark CI, Pike GB. Indication of BOLD-specific venous flow-volume changes from precisely controlled hyperoxic vs. hypercapnic calibration. J Cereb Blood Flow Metab. 2012; 32:709–719. [PubMed: 22167238]

Moosmann M, Ritter P, Krastel I, Brink A, Thees S, Blankenburg F, Taskin B, Obrig H, Villringer A. Correlates of alpha rhythm in functional magnetic resonance imaging and near infrared spectroscopy. Neuroimage. 2003; 20:145–158. [PubMed: 14527577]

Mulderink TA, Gitelman DR, Mesulam MM, Parrish TB. On the use of caffeine as a contrast booster for BOLD fMRI studies. Neuroimage. 2002; 15:37–44. [PubMed: 11771972]

Murphy K, Birn RM, Handwerker DA, Jones TB, Bandettini PA. The impact of global signal regression on resting state correlations: are anti-correlated networks introduced? Neuroimage. 2009; 44:893–905. [PubMed: 18976716]

Ogawa S, Menon RS, Tank DW, Kim SG, Merkle H, Ellerman JM, Ugurbil K. Functional brain mapping by blood oxygenation level—dependent contrast magnetic resonance imaging: a comparison of signal characteristics with a biophysical model. Biophys J. 1993; 64:803–812. [PubMed: 8386018]

Olbrich S, Mulert C, Karch S, Leicht G, Pogarell O, Hegerl U. EEG-vigilance and BOLD effect during simultaneous EEG/fMRI measurement. Neuroimage. 2009; 45:319–332. [PubMed: 19110062]

Pelligrino DA, Xu HL, Vetri F. Caffeine and the control of cerebral hemodynamics. J Alzheimers Dis. 2010; 20(Suppl. 1):S51–S62. [PubMed: 20182032]

Peltier SJ, Shah Y. Biophysical modulations of functional connectivity. Brain Connect. 2011; 1:267–277. [PubMed: 22432417]

Rack-Gomer, AL. Bioengineering. University of California San Diego; La Jolla: 2011. Baseline Effects on Resting-State Functional Connectivity; p. 99

Rack-Gomer AL, Liau J, Liu TT. Caffeine reduces resting-state BOLD functional connectivity in the motor cortex. Neuroimage. 2009; 46:56–63. [PubMed: 19457356]

Restom K, Perthen JE, Liu TT. Calibrated fMRI in the medial temporal lobe during a memory-encoding task. Neuroimage. 2008; 40:1495–1502. [PubMed: 18329291]

Ritter P, Moosmann M, Villringer A. Rolandic alpha and beta EEG rhythms' strengths are inversely related to fMRI-BOLD signal in primary somatosensory and motor cortex. Hum Brain Mapp. 2008; 30:1168–1187. [PubMed: 18465747]

Scheeringa R, Bastiaansen MC, Petersson KM, Oostenveld R, Norris DG, Hagoort P. Frontal theta EEG activity correlates negatively with the default mode network in resting state. Int J Psychophysiol. 2008; 67:242–251. [PubMed: 17707538]

Shin, DD.; Liu, HL.; Wong, EC.; Liu, TT. Effect of background suppression on CBF quantitation in pseudo continuous arterial spin labeling; 19th Annual ISMRM Scientific Meeting; Montreal. 2011. p. 2101

Siepmann M, Kirch W. Effects of caffeine on topographic quantitative EEG. Neuropsychobiology. 2002; 45:161–166. [PubMed: 11979068]

Smith AJ, Blumenfeld H, Behar KL, Rothman DL, Shulman RG, Hyder F. Cerebral energetics and spiking frequency: the neurophysiological basis of fMRI. Proc Natl Acad Sci U S A. 2002; 99:10765–10770. [PubMed: 12134056]

Sorg C, Riedl V, Muhlau M, Calhoun VD, Eichele T, Laer L, Drzezga A, Forstl H, Kurz A, Zimmer C, Wohlschlager AM. Selective changes of resting-state networks in individuals at risk for Alzheimer's disease. Proc Natl Acad Sci U S A. 2007; 104:18760–18765. [PubMed: 18003904]

Stamatakis EA, Adapa RM, Absalom AR, Menon DK. Changes in resting neural connectivity during propofol sedation. PLoS One. 2010; 5:e14224. [PubMed: 21151992]

Tal O, Diwakar M, Wong CW, Olafsson V, Lee R, Huang MX, Liu TT. Caffeine-induced global reductions in resting-state BOLD connectivity reflect widespread decreases in MEG connectivity. Front Hum Neurosci. 2013; 7(63):1–10. [PubMed: 23355817]

Thomason ME, Foland LC, Glover GH. Calibration of BOLD fMRI using breath holding reduces group variance during a cognitive task. Hum Brain Mapp. 2007; 28:59–68. [PubMed: 16671081]

Veselis RA, Feshchenko VA, Reinsel RA, Beattie B, Akhurst TJ. Propofol and thiopental do not interfere with regional cerebral blood flow response at sedative concentrations. Anesthesiology. 2005; 102:26–34. [PubMed: 15618783]

Wang L, Zang Y, He Y, Liang M, Zhang X, Tian L, Wu T, Jiang T, Li K. Changes in hippocampal connectivity in the early stages of Alzheimer's disease: evidence from resting state fMRI. Neuroimage. 2006; 31:496–504. [PubMed: 16473024]

Wang K, Liang M, Wang L, Tian L, Zhang X, Li K, Jiang T. Altered functional connectivity in early Alzheimer's disease: a resting-state fMRI study. Hum Brain Mapp. 2007; 28:967–978. [PubMed: 17133390]

Weissenbacher A, Kasess C, Gerstl F, Lanzenberger R, Moser E, Windischberger C. Correlations and anticorrelations in resting-state functional connectivity MRI: a quantitative comparison of preprocessing strategies. Neuroimage. 2009; 47:1408–1416. [PubMed: 19442749]

Wong CW, Olafsson V, Tal O, Liu TT. Anti-correlated networks, global signal regression, and the effects of caffeine in resting-state functional MRI. Neuroimage. 2012; 63:356–364. [PubMed: 22743194]

Wong, CW.; Olafsson, V.; Tal, O.; Liu, TT. Caffeine-induced reductions in the resting-state fMRI global signal reflect increases in EEG vigilance measures; 21st Annual ISMRM Scientific Meeting; Salt Lake City. 2013. p. 33

Wu CW, Gu H, Lu H, Stein EA, Chen JH, Yang Y. Mapping functional connectivity based on synchronized $CMRO_2$ fluctuations during the resting state. Neuroimage. 2009; 45:694–701. [PubMed: 19280693]

Xu F, Uh J, Brier MR, Hart J, Yezhuvath US, Gu H, Yang Y, Lu H. The influence of carbon dioxide on brain activity and metabolism in conscious humans. J Cereb Blood Flow Metab. 2011; 31:58–67. [PubMed: 20842164]

Zappe AC, Uluda K, Oeltermann A, U urbil K, Logothetis NK. The influence of moderate hypercapnia on neural activity in the anesthetized nonhuman primate. Cereb Cortex. 2008; 18:2666–2673. [PubMed: 18326521]

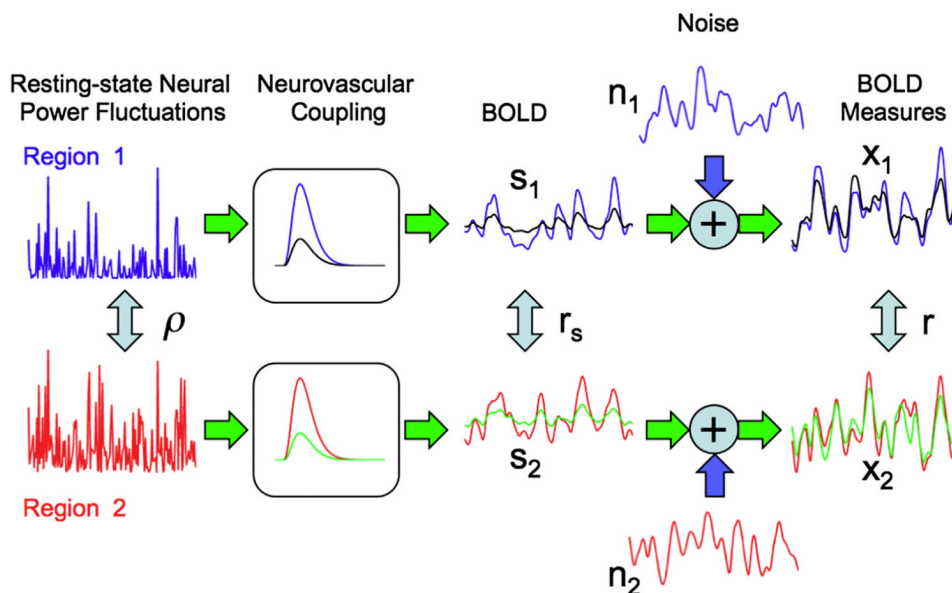**Fig. 1.**
The correlation r between the measured BOLD time series (x_1 and x_2) from two different brain regions depends on the neurovascular coupling pathway. The measured BOLD time series in each region can be viewed as the sum of a BOLD component (s_1 and s_2 for regions 1 and 2, respectively) and a noise component (n_1 and n_2, respectively), where the BOLD component is obtained by convolving the neural power fluctuations (blue and red time courses on the left) with the hemodynamic response functions. The correlation between the underlying neural power fluctuations is designated as ρ. For the blue and red hemodynamic responses, the resultant BOLD components and measures are shown by the blue and red time series, respectively, with a correlation value of $r = 0.54$ between the measured BOLD time series. For a change in neurovascular coupling that reduces the amplitudes of the hemodynamic responses by one third (indicated by the black and green hemodynamic responses), there is a decrease (by one third) in both the amplitudes of the BOLD component time series and the SNR of the measured BOLD time series (black and green lines). With the SNR decrease, the correlation of the measured BOLD time series drops to $r = 0.41$.
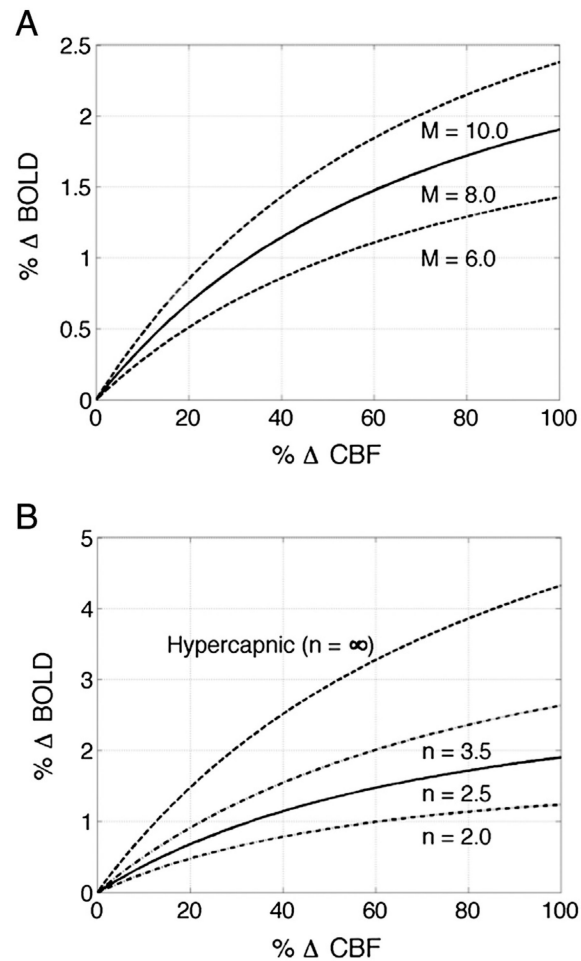
Fig. 2.
Plots of the percent BOLD versus percent CBF response amplitudes computed with the BOLD signal model presented in Eq. (1). (A) Percent BOLD versus percent CBF responses for different values of the parameter M and a fixed coupling parameter of $n = 2.5$. As the parameter M increases, the BOLD signal increases more rapidly for a given change in CBF. (B) Percent BOLD versus percent CBF responses for different values of the coupling parameter n and a fixed M parameter value of 8.0%. As the coupling parameter decreases, the CBF and $CMRO_2$ responses become more tightly coupled and the BOLD response decreases.
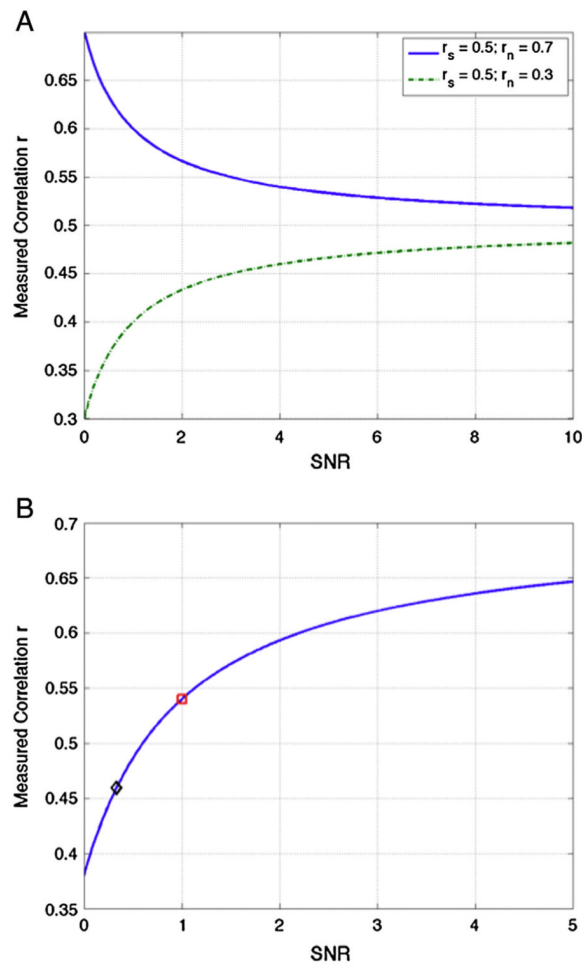
Fig. 3.
(A) The measured correlation $r = r_s(SNR + (r_n/r_s))/(SNR + 1)$ exhibits a dependence on SNR that depends on the relative relation between the source correlation r_s and the noise correlation r_n. As SNR increases the measured correlation approaches the source correlation value r_s, and as SNR decreases the measured correlation approaches the noise correlation value r_n. The dashed green line and solid blue line show the dependence when the noise correlation is lower ($r_n = 0.3$) or higher ($r_n = 0.7$), respectively, than the source correlation ($r_s = 0.5$). (B) Correlation as a function of SNR for the signals shown in Fig. 1. For the larger hemodynamic responses (blue and red responses in Fig. 1), the SNR is equal to 1 and the measured correlation of $r = 0.54$ is indicated by the red square. With a reduction in the amplitude of hemodynamic responses(black and green responses in Fig. 1), the SNR drops to 0.33 and the measured correlation of $r = 0.41$ is indicated by the black diamond.
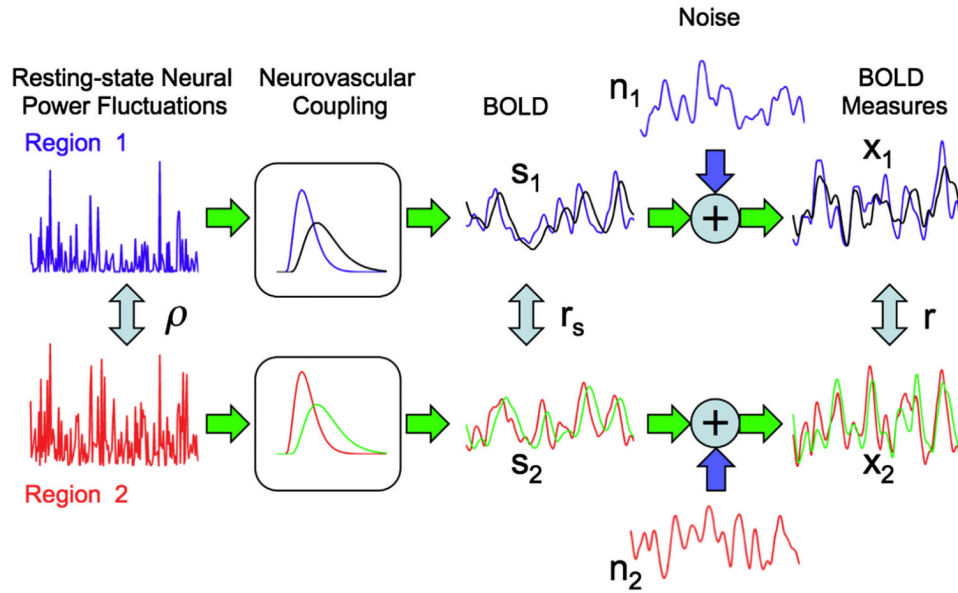
Fig. 4.
Effect of changes in the shape of the hemodynamic response on the correlation between the measured BOLD time series. The blue and red hemodynamic responses and the corresponding BOLD component and measured time series (also in blue and red) are identical to those depicted in Fig. 1. For this condition, the signal and noise correlations are $r_s = 0.70$ and $r_n = 0.38$ and the measured correlation is $r = 0.54$. With an overall slowing down of the hemodynamic responses (shown in black and green), the BOLD component time courses become delayed and smoother (black s_1 and green s_2) as compared to the original time courses (blue s_1 and red s_2), and the signal correlation drops to $r_s = 0.63$. The noise time courses remain unchanged, but the measured BOLD time series (black x_1 and green x_2) are altered, with a correlation value of $r = 0.34$. The decrease in correlation is even more pronounced if the hemodynamic response from one region changes while the other remains the same. For example, if the region 1 response is unchanged (blue hemo-dynamic response) while the region 2 response slows down (green hemodynamic response), the correlation value drops to $r = 0.17$ (reflecting the correlation between blue x_1 and green x_2).